Supporting information for

Significantly improved photovoltaic performance of the triangular-spiral TPA(DPP-PN)₃ by appending planar phenanthrene units into the molecular terminals

Youming Zhang,[a] Xichang Bao,*[b] Manjun Xiao,[a,b] Hua Tan,*[a,c] Qiang Tao,[a] Yafei Wang,[a] Yu Liu,[a] Renqiang Yang*[b] and Weiguo Zhu*[a]

*a*College of Chemistry, Xiangtan University, Key Lab of Environment-Friendly Chemistry and Application in Ministry of Education, Xiangtan 411105, China

*b*Qingdao Institute of Bioenergy and Bioprocess Technology, Chinese Academy of Sciences, Qingdao, Shandong 266101, China

c Institute of Polymer Optoelectronic Materials and Devices, State Key Laboratory of Luminescent Materials and Devices, South China University of Technology, Guangzhou 510640, China

* Corresponding authors. Tel.: +86-731-58293377; fax: +86-731-58292251(W. Zhu).

Email addresses:

(W. Z.) zhuwg18@126.com,

(R. Y.) yangrq@qibebt.ac.cn,

(X. B.) baoxc@qibebt.ac.cn,

(H. T) tanhua815@126.com.

1. General considerations for characterization

Instrument: Nuclear magnetic resonance (NMR) spectra were recorded on a Bruker DRX 400 spectrometer using tetramethylsilane as a reference in deuterated chloroform solution at 298 K. MALDI-TOF mass spectrometric measurements were performed on Bruker Bifiex III MALDI-TOF. Thermogravimetric analysis (TGA) was conducted under a dry nitrogen gas flow at a heating rate of 10 $^{\circ}$C min^{-1} on a Perkin- Elmer TGA 7. UV-Vis absorption spectra were recorded on a HP-8453 UV visible system. Cyclic voltammetry was carried out on a CHI660A electrochemical work station in a three-electrode cell dipped in a 0.1M tetrabutylammonium hexafluoro- phosphate (Bu$_4$NPF$_6$) acetonitrile solution under nitrogen protection at a scan rate of 100 mV/s and room temperature (RT). In this three-electrode cell, a platinum rod, platinum wire and Ag/AgCl electrode were used as a working electrode, counter electrode and reference electrode, respectively.

Device fabrication and characterization: OSCs were fabricated using indium tin oxide (ITO) glass as an anode, Ca(10 nm)/Al(100 nm) as a cathode, and a blend film of the small molecules and [6,6]-phenyl-C61 (or C71)-butyric acid methyl ester (PCBM) as a photosensitive layer. After a 30 nm buffer layer of poly- (3,4-ethylene-dioxythiophene) and polystyrene sulfonic acid (PEDOT: PSS) was spin-coated onto the precleaned ITO glass, the photosensitive layer was subsequently prepared by spin-coating a solution of the polymer and PCBM (1:2.5, *w/w*) in chloroform on the PEDOT:PSS layer with a typical concentration of 10 mg mL^{-1}, followed by annealing at 50 $^{\circ}$C for 10 minutes to remove chloroform. Ca (10 nm) and Al (100 nm) were successively deposited on the photosensitive layer in vacuum and used as top

electrodes. The current density-voltage (J-V) characteristics were recorded with a Keithley 2420 source measurement unit under simulated 100 mW cm^{-2} (AM 1.5G) irradiation from a Newport solar simulator. Light intensity was calibrated with a standard silicon solar cell. The external quantum efficiencies (EQE) of solar cells were analyzed using a certified Newport incident photon conversion efficiency ($IPCE$) measurement system.

Hole mobility of the molecules (1:2.5, *w/w*) blend film was measured according to a similar method described in the literature[1-2], using a diode configuration of ITO/PEDOT:PSS(40nm)/active layer (180 or 230 nm)/Ca(10 nm)/Al(100 nm) MoO$_3$ (5 nm)/Ag (80 nm) by taking current-voltage current in the range of 0 - 4 V and fitting the results to a space charge limited form, where the space charge limited current (SCLC) is described by $J = 9\varepsilon_0\varepsilon_r\mu_h V^2/8L^3$, where J is the current density, L is the film thickness of active layer, μ_h is the hole mobility, ε_r is the relative dielectric constant of the transport medium, ε_0 is the permittivity of free space (8.85 × 10^{-12} F m^{-1}), V is the internal voltage in the device and $V = V_{appl}$-V_a-V_{bi}, where V_{appl} is the applied voltage to the device, V_a is the voltage drop due to contact resistance and series resistance across the electrodes, and V_{bi} is the built-in voltage due to the relative work function difference of the two electrodes.

## 2. Photovoltaic Properties of the TPA(DPP-PN)₃ based OSCs at different conditions
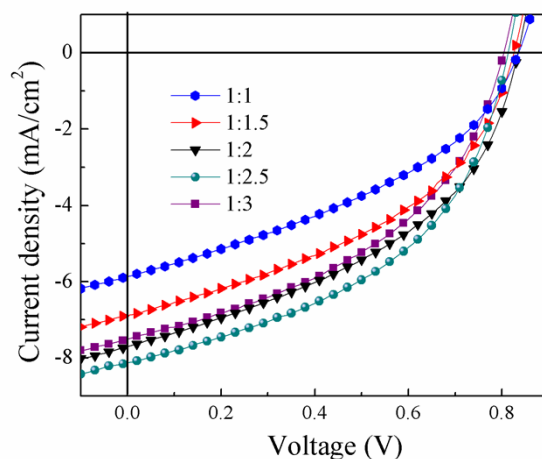
Figure S1. Current–voltage (J–V) curves of BHJ solar cells with the TPA(DPP-PN)$_3$/PC$_{61}$BM blends at various weight ratios under AM 1.5G illumination (100 mW cm^{-2}).

Table S1. Photovoltaic properties of BHJ solar cell devices with a configuration of ITO/PEDOT: PSS/ TPA(DPP-PN)$_3$:PC$_{61}$BM/Ca/Al[a]

TPA(DPP-P)$_3$:PC$_{61}$BM	V_{oc}/ V	J_{sc}/ mA cm^{-2}	FF/ %	PCE$_{max}$/ %
1:1	0.83	5.86	38.99	1.90
1:1.5	0.82	6.88	43.21	2.45
1:2	0.83	7.69	43.90	2.82
1:2.5	0.81	8.12	46.62	3.07
1:3	0.80	7.50	44.21	2.66

[a] Measured under AM 1.5 G irradiation (100 mW cm^{-2}).
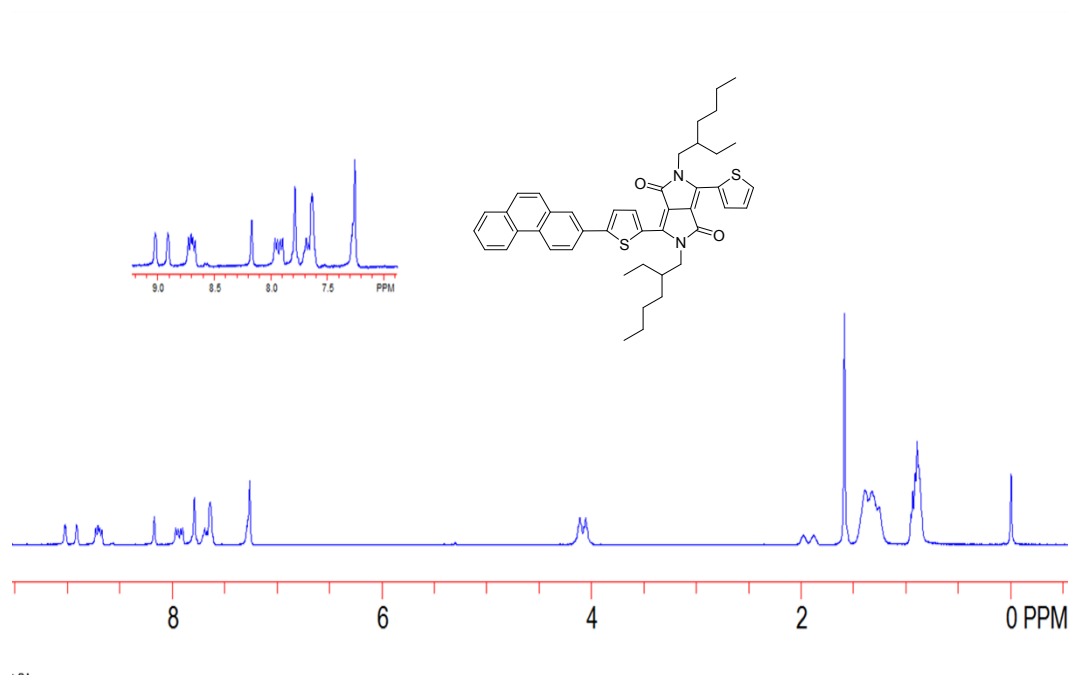
3. Film morphology
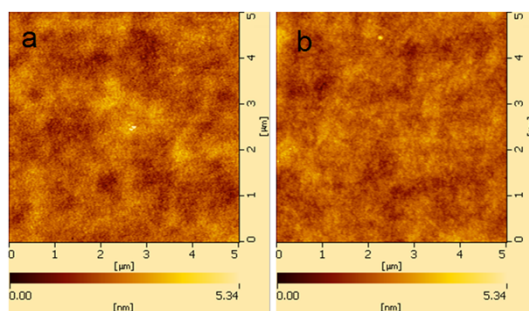
Figure S2. Tapping-mode AFM images of the blended films of TPA-3DPP/PC$_{71}$BM (a) and TPA(DPP-PN)$_3$/PC$_{71}$BM (b) on glass/ITO/PEDOT:PSS substrate.
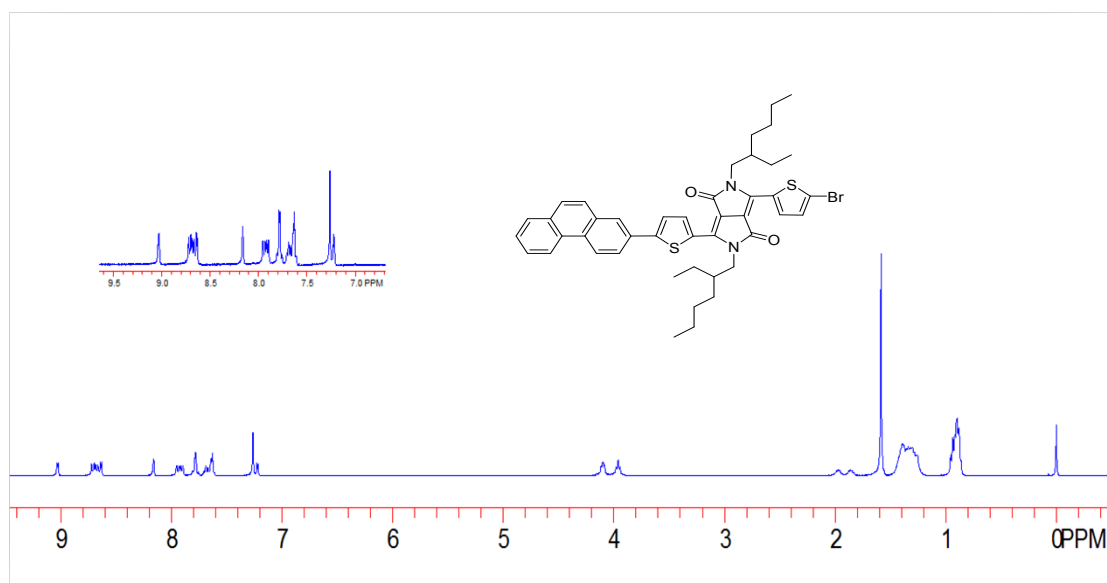
4. ^{1}H NMR and MS profiles of PN-BPin, PN-DPP, PN-DPP-Br, TPA-3BPin, TAP-3DPP and TPA(DPP-PN)$_3$.
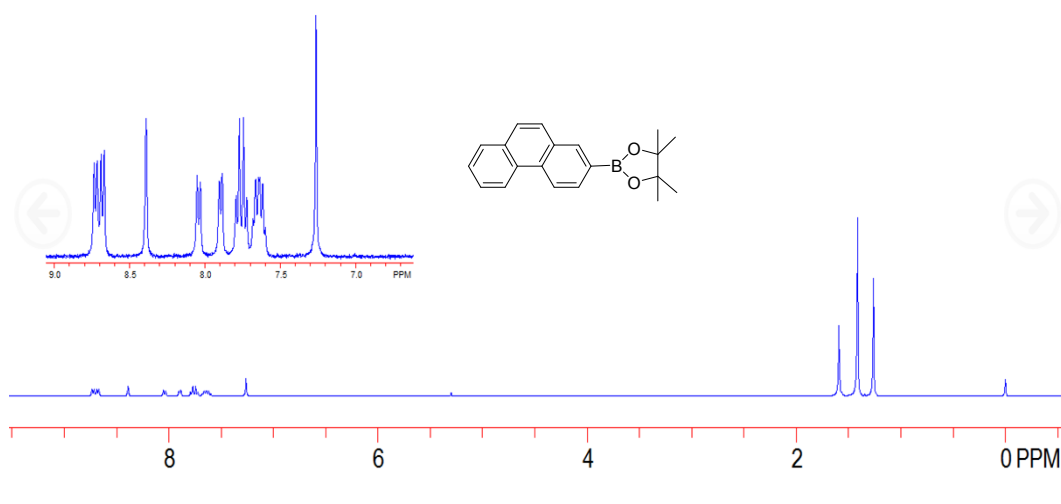
Figure S3-1. ^{1}H NMR profile of PN-BPin

Figure S3-2. ^{1}H NMR profile of PN-DPP
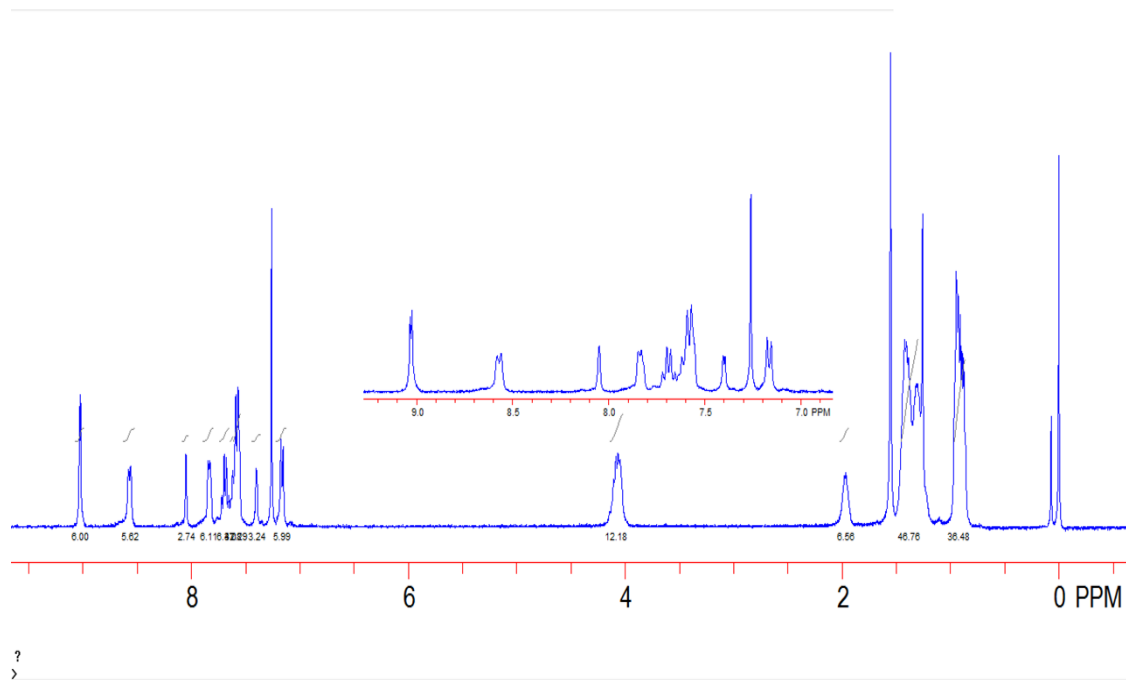

Figure S3-3. ^{1}H NMR profile of PN-DPP-Br

Figure S3-4. ¹H NMR profile of TPA-3BPin

Figure S3-5. ¹H NMR profile of TPA-3DPP

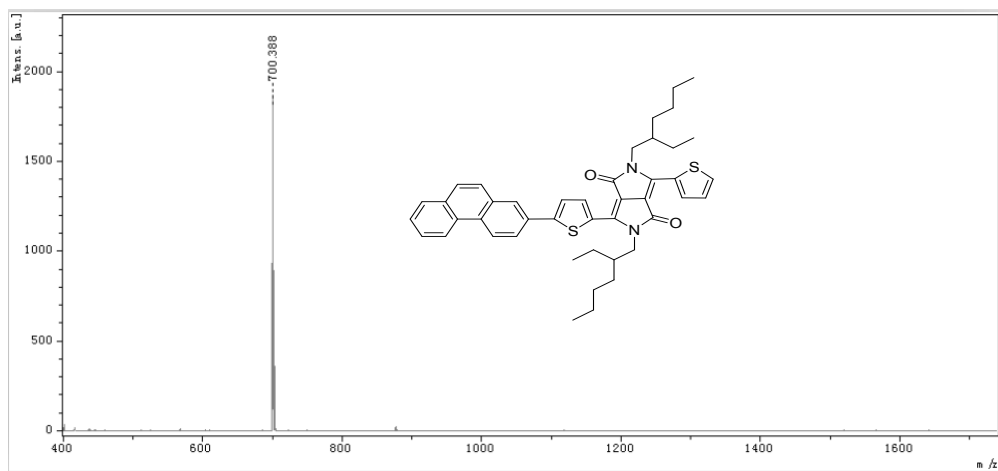**Figure S3-6.** ^{1}H NMR profile of TPA(DPP-PN)$_3$

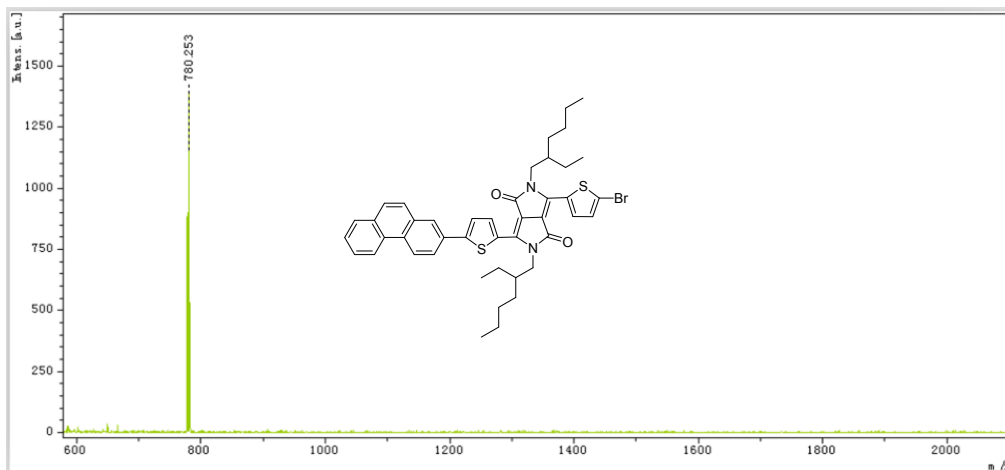**Figure S3-7.** MS profile of PN-DPP

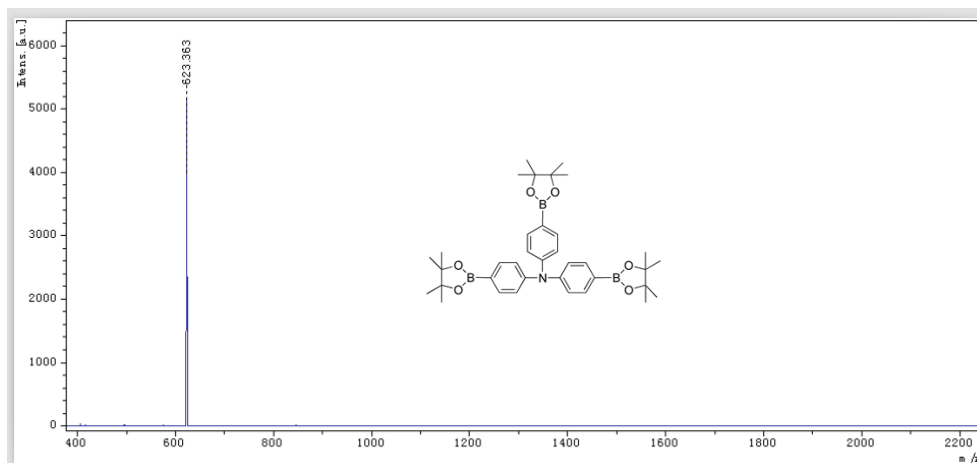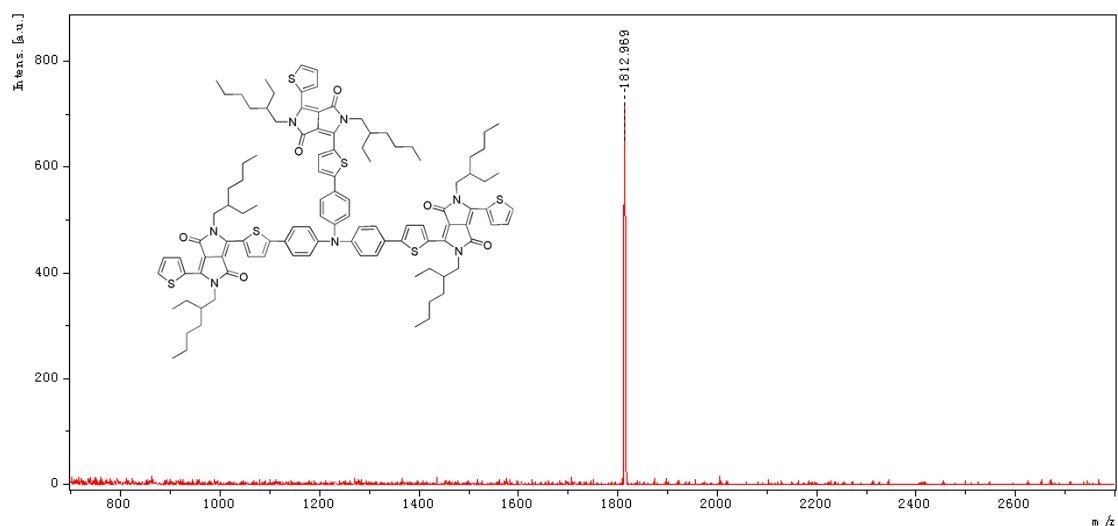**Figure S3-8.** MS profile of PN-DPP-Br
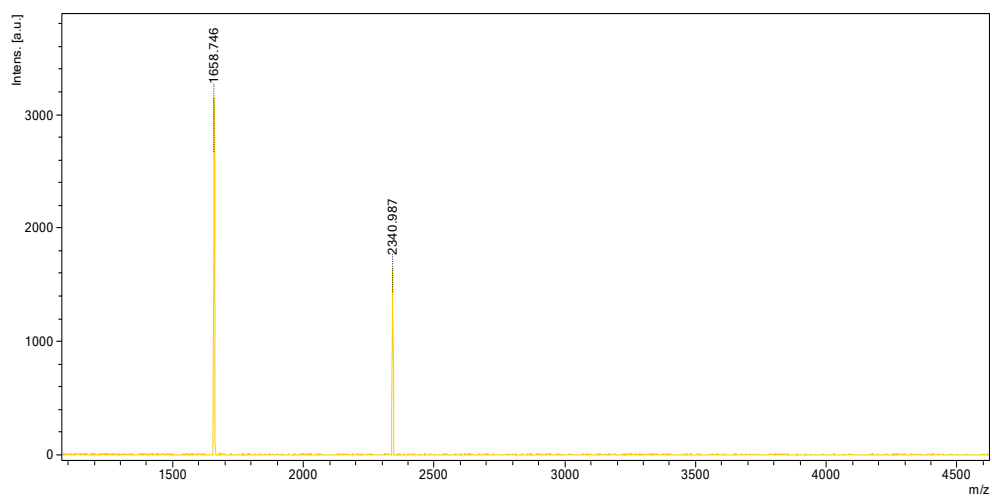

Figure S3-9. MS profile of TPA-3BPin

Figure S3-10. MS profile of TPA-3DPP

Figure S3-11. MS profile of TPA(DPP-PN)$_3$

Reference

[1]. M. Wang, X.W. Hu, P. Liu, W. Li, X. Gong, F. Huang, Y. Cao, *J. Am. Chem. Soc*. 2011**, 133**, 9638.

[2]. Z.C. He, C.M. Zhong, X. Huang, W.Y. Wong, H.B. Wu, L.X. Chen, Y. Cao, *Adv. Mater*. 2011, **23**, 4636.